



1-(2-Hydroxyethyl)-2-imidazolidinone as corrosion inhibitor of mild steel in 0.5 M HCl solution: thermodynamic, electrochemical and theoretical studies

Ayşen Keleşoğlu, Reşit Yıldız & İlyas Dehri

To cite this article: Ayşen Keleşoğlu, Reşit Yıldız & İlyas Dehri (2019): 1-(2-Hydroxyethyl)-2-imidazolidinone as corrosion inhibitor of mild steel in 0.5 M HCl solution: thermodynamic, electrochemical and theoretical studies, Journal of Adhesion Science and Technology, DOI: [10.1080/01694243.2019.1623967](https://doi.org/10.1080/01694243.2019.1623967)

To link to this article: <https://doi.org/10.1080/01694243.2019.1623967>



Published online: 13 Jun 2019.



Submit your article to this journal [↗](#)



View Crossmark data [↗](#)



1-(2-Hydroxyethyl)-2-imidazolidinone as corrosion inhibitor of mild steel in 0.5 M HCl solution: thermodynamic, electrochemical and theoretical studies

Ayşen Keleşoğlu^a, Reşit Yıldız^b and İlyas Dehri^a

^aDepartment of Chemistry, Çukurova University, Adana, Turkey; ^bHealth Sciences Faculty, Department of Nutrition and Dietetics, Mardin Artuklu University, Mardin, Turkey

ABSTRACT

The inhibition effect of 1-(2-Hydroxyethyl)-2-imidazolidinone (2-HEI) on mild steel (MS) corrosion in 0.5 M HCl solution was investigated at different inhibitor concentration and temperature by electrochemical experiments, such as linear polarization resistance (LPR), electrochemical impedance spectroscopy (EIS), potentiodynamic polarization and quantum chemical calculations. The inhibitor adsorption process on mild steel in 0.5 M HCl system was studied at different temperatures (20 °C–50 °C). Furthermore, the surface morphology of MS was also investigated with SEM in the absence and the presence of inhibitor. The adsorption of 1-(2-Hydroxyethyl)-2-imidazolidinone on MS surface is an exothermic process and this process obeys the Langmuir adsorption isotherm. The Quantum chemical findings are good agreed with the empirical data.

ARTICLE HISTORY

Received 2 April 2019
Revised 19 May 2019
Accepted 21 May 2019

KEYWORDS

Interfaces; electrochemical techniques; corrosion inhibitor; SEM; quantum chemical calculation; adsorption

1. Introduction

MS is an alloy of Fe, which is used in structural and industrial practises due to its outstanding mechanical properties particulars. Acid solutions handle it, and generally, it undergoes dissolution in acidic solutions. Corrosion control approaches were used to abstain from the MS dissolution of acidic solutions [1]. Inhibitors are the heterocyclic structures, which are having heteroatoms such as O, N, S, P and π electrons in their heterocyclic ring system. Through these, inhibitor structures can get adsorbed on the surface of MS [2–4].

Heterocyclic structures like benzimidazole derivatives [5,6], triazole derivatives [7,8], thiosemicarbazide derivatives [9], bisthiadiazoles [10], Schiff base [11], organic dyes [12–17] and pyridine derivatives [18–24] have been tested as influential corrosion inhibitors for MS. Researchers have paid interest to the drugs development as inhibitors for MS corrosion. The offer examine focussed on the inhibition effect of

1-(2-Hidroksietil)-2-İmidazolidion on corrosion of MS in 0.5 M HCl. The study took place at different concentrations with the raised temperature range of 20 C–50 °C.

1-(2-Hydroxyethyl)-2-imidazolidinone (2-HEI) has adsorption centers such as –OH group; –N and O heteroatoms, NH– group and aromatic rings in its molecule and may be assist its adsorption on the MS surface for the investigation of inhibition influence.

The corrosion inhibition effect of 2-HEI is examined by electrochemical measurements. i.e. Tafel polarization, LPR and EIS measurements for MS in 0.5 M HCl. The surface morphology is studied by SEM and in theory this examine is ustifiable by utilizer Quantum chemical assay by DFT methods.

2. Experimental

2.1. Preparation of electrode

The MS, whose composition is known ((wt%) P (0.045%), C(0.17%), N (0.009%) Mn (1.40%), S (0.045%) and Fe (98,376)) and which is about 4 cm in length, is covered with a polyester made with a metallic connection with a copper wire and the other surface exposed. Working surface; the exposed surface is 0.5 cm². Before all measurements, the working surface of the electrode was polished using a mechanical polish with different particle size sand paper (The MS specimen surface was abraded with abrasive papers starting from 100 to 1200 grit size.) and cleaned with pure water and dried in air, then followed by acetone degreasing before immersing in the solution.

2.2. Test solutions

The working medium at 20 °C contains 0.5 M HCl (37% HCl (MERCK, Art. 317)) solution and solutions containing 1-(2-hydroxyethyl)-2-imidazolidione (2-HEI) at concentrations of 0.5 mM, 1 mM, 5 mM, and 10 mM. The 2-HEI structure is given in [Figure 1](#). In each experiment, a freshly prepared solution was used. A temperature range of 20–50 °C was made for solutions containing 0.5 M HCl solution and 2-HEI at a constant concentration of 10 mM.

2.3. Electrochemical measurements

The EIS measurements were performed in 0.5 M HCl solution and containing various concentrations of 2-HEI at 20 °C on MS that is 0.5 cm² surface area after steady state condition was ensured for 30 min without de-aeration of the solution. A conventional three-electrode system was connected to an electrochemical CHI 604 A (potentiostat/galvanostat (serial number: 6A721A) for all EIS measurements. The working electrode

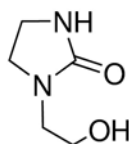


Figure 1. 1-(2-Hydroxyethyl)-2-imidazolidinone (2-HEI).

(MS), a counter electrode (platinum (2 cm² surface area)) and a reference electrode (Ag/AgCl (3 M KCl)) were used for the analyses. The counter electrode was a platinum electrode, and a Ag/AgCl (3 M KCl) electrode was used as a reference. Prior to the implementation of the test, it was necessary to reach a stable potential state; therefore, the electrode was immersed in the test solution for 30 minutes at open circuit potential to achieve steady state condition. The measurements of EIS were then fulfilled in the OCP by applying a signal with a perturbation of 10 mV peak to peak in a frequency range from 10⁵ Hz to 10⁻² Hz.

LPR Measurements: The corrosion potential was initiated at a value of 10 mV lower and the range of up to 10 mV was more positive than the one obtained by scanning at a scan rate of 1 mV/s. The R_p was derived from the slope of the acquired potential-current curves.

The PD curves were obtained from a cathodic potential of -1.000 V(Ag/AgCl) to an anodic potential of -0.100 V(Ag/AgCl) versus Ag/AgCl (3 mol L⁻¹ KCl) with respect to the E_{ocp} . The scanning speed was 1 mV/s.

2.4. Sem studies

Surface investigation of MS was fulfilled by using scanning electron microscope (a Carl Zeiss Evo 40 model). The micrographs of MS surface were recorded after 120 h exposing the uninhibitor and 10 mM 2-HEI comprising 0.5 M HCl test solutions.

2.5. Quantum chemical calculations

Quantum chemical calculations were carried out by complete geometry optimization using standard Gaussian 03 programme package (USA). The molecular structure of the 2-HEI molecule was optimized by DFT with the 6-311++G(d,p) basis set of orbitals of atomic as exercised in the programme package of Gaussian 03 [25,26].

3. Results and discussion

3.1. Change of open circuit potential with exposure period

Figure 2 presents the variation of the E_{ocp} of the MS with time in 0.5 M HCl solution in the absence and presence of 0.5 mM–10 mM 2-HEI at 25 °C. Seemingly, E_{ocp} remains nearly unrevised after 60 min (in absence of 2-HEI it was -0.507 V (vs. Ag/AgCl, 3 M KCl) and in the presence of 10 mM 2-HEI it was -0.476 V (vs. Ag/AgCl, 3 M KCl)), which is demonstrative of the steady state.

3.2. Potentiodynamic polarization measurements

The polarization behavior of MS in 0.5 M HCl in the presence and absence of different inhibitor concentrations under investigation is expensed in Figure 3(a,b). It is established that i_{corr} values decreased a good many in inhibitor presence and diminished with augmenting inhibitor concentration while E_{corr} values were remain nearly unchanged.

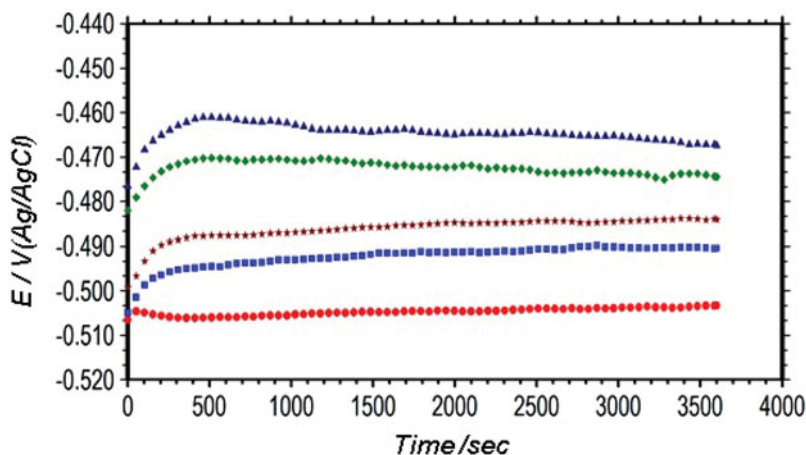


Figure 2. The open circuit potential–time curves of MS obtained in 0.5 M HCl (●) solution containing various concentrations (0.5 mM (■), 1.0 mM (*), 5.0 mM (◆) and 10.0 mM (▲)) of 2-HEI.

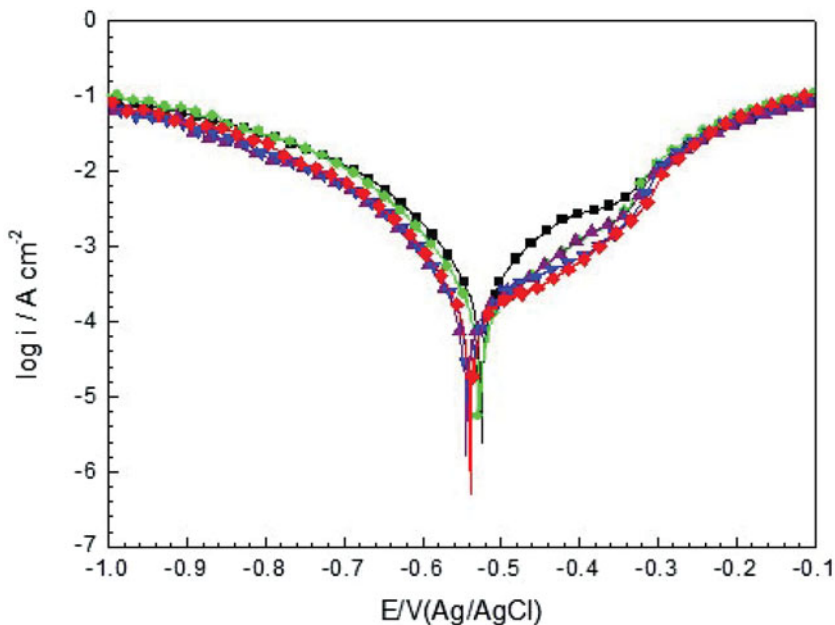


Figure 3. Potentiodynamic polarization curves of MS electrode obtained in 0.5 M HCl solution (▲) and containing 0.5 (▲), 1.0 (◆), 5.0 (■) and 10.0 mM (●) 2-HEI at 20 °C.

From the polarization plots, it is explicated that both cathodic hydrogen evolution reaction and anodic metal dissolution were inhibited after the supplement by 2-HEI to both acid solutions. This means that the supplement by 2-HEI modifies barely cathodic and anodic slopes. The curves of Tafel lines almost remained the same display the inhibitive action to represent adsorption of inhibitor structures on the MS surface and engorging of active zones [27].

PD curves for MS in 0.5 M HCl with and without 2-HEI are epitomised in [Figure 3](#). As it can be seen from the figure, addition of the 2-HEI affected the cathodic and

anodic parts of the PD curve diagnosis that the 2-HEI is a mixed-type inhibitor. Therewithal, the anodic and cathodic density of current also decreased with the increasing corrosion inhibitor concentrations [28]. Furthermore in Figure 3, the observed E_{corr} values were; -508 , -490 , -485 , -484 , -475 mV for 0, 0.5, 1, 5, 10 mM 2-HEI continuing media, respectively.

As the anodic potential curves do not have linear Tafel fields, the current density of corrosion and efficiencies of inhibition could not be calculated from the parameters obtained from the Tafel slopes in the anodic and cathodic directions. For this reason, i_{corr} values were determined by exploiting equation of Stern Geary;

$$i_{corr} = B/R_p \quad (1)$$

where R_p is the resistance of polarization which were specified from impedance data, B is 0.026 V [29]. The determined values were 5.26×10^{-5} A cm^{-2} , 8.44×10^{-5} , 9.2×10^{-5} , 10.4×10^{-5} and 36.1×10^{-5} for 10, 5, 1, 0.5, and 0 mM 2-HEI including media, respectively. As it can be seen obviously, the calculated values were diminished with augmenting 2-HEI concentration. The inhibition process of 2-HEI was recommended consequently an immobilisation mechanism of the actives zones on surface, which can occur by physical and/or chemical adsorption. Similar results for imidazolidinone derivates were reported in the literature. Tang et al. [5] reported that inhibition efficiencies of MS corrosion increased by increasing of 2-aminomethyl benzimidazole (ABI), bis (2-benzimidazolylmethyl) amine (BBIA) and tri (2-benzimidazolylmethyl) amine (TBIA) concentrations. These values were 74.15, 92.19 and 94.14% for 2 mM ABI, BBIA and TBIA in 1.0 M HCl solution according to potentiodynamic techniques, respectively. Aljourani et al. [6] studied the corrosion inhibition effect of benzimidazole, 2-methylbenzimidazole and 2-mercaptobenzimidazole on the MS in 1.0 M HCl solution. The corrosion inhibition efficiencies were found to be 52.2, 57.1 and 88.7% at 250 ppm of inhibitors, respectively.

3.3. EIS measurements

Figure 4(a,b) indicate the Bode and Nyquist curves for MS in 0.5 M HCl without and with different concentrations of inhibitor. It is indicated from this curves that EIS reply of MS in both acids has comparatively altered later the make addition of inhibitor. As can be seen obviously in Figure 4(a,b), Nyquist curves are decadent into the real axis and not excellent hemicycle as awaited from theory of EIS for reputed circuit of equivalent and this is always attributed to the roughness, impurities, grain boundaries, distribution of surface active sites and inhomogeneity of the MS surface ascent from surface snafu or interfacial phenomena. The ideal capacitive behavior is not seen in this case and hence a constant phase element CPE is introduced in the circuit to give a more accurate fit [30–33]. The consequences defined subjacent can be explicated in the way of equivalent circuit of the electrical double layer displayed in Figure 5 [34]. The value of R_{ct} have been estimated from the difference in EIS at lower and higher frequencies [35]. The values of C_{dl} were determined using the following relation:

$$C_{dl} = Y_o(w_{max})^{n-1} \quad (2)$$

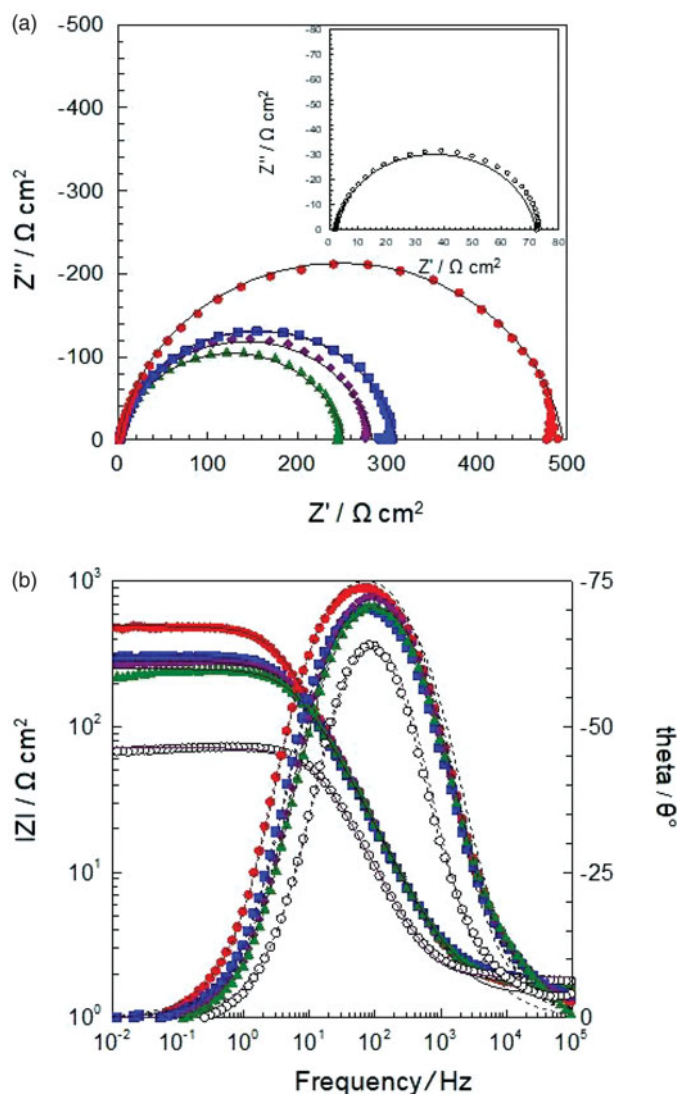


Figure 4. Nyquist (a) and Bode (b) plots of MS electrode obtained in 0.5M HCl solution (\wedge) (inset) and containing 0.5 (\blacktriangle), 1.0 (\blacklozenge), 5.0 (\blacksquare) and 10.0 mM (\bullet) 2-HEI (solid lines show fitted results).

where $w_{max} = 2\Pi f_{max}$. The Cdl value is the relation to the frequency at which the imaginary component of impedance is maximum (f_{max}) [36].

Electrical equivalent circuit diagram (Figure 5) generally used for modeling metal/solution interface [37–40].

The use of CPE instead of double layer capacitance (Cdl) could be linked to a more accurate fit in the case of deviation from an ideal capacitor as a result of different physical phenomena like surface roughness, inhibitor adsorption, porous layer formation, etc. The double layer capacitance value, but, provides a better validation of the equivalent circuit model and can be determined from the CPE according to the following equation [26,41–43]:

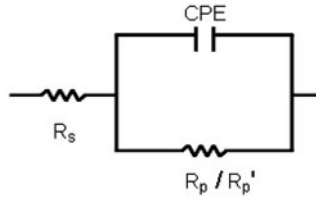


Figure 5. Electrical equivalent circuit diagrams used to modeling metal/solution interface. R_s : solution resistance, R_p : polarization resistance, CPE : double layer capacitance and film capacitance for uninhibited and inhibited solutions, respectively. R_p corresponds to charge transfer resistance (R_{ct}) and diffuse layer resistance (R_d) at the metal/solution interface in the absence of inhibitor ($R_p = R_{ct} + R_d$). R_p' includes the accumulated species (R_d), R_p and film resistance (R_f), ($R_p' = R_p (R_{ct} + R_d) + R_a + R_f$).

Table 1. Electrochemical parameters of MS in 0.5 mol L⁻¹ HCl solution in the absence and presence of different concentration of 2-HEI.

C_{inh} (mM)	EIS						LPR		
	E_{corr} (mV)	R_s (Ω cm ²)	R_p (Ω cm ²)	CPE ($\times 10^6$ s ⁿ Ω^{-1} cm ⁻²)	n	η (%)	C_{dl} ($\times 10^6$ s Ω^{-1} cm ⁻²)	R_p (Ω cm ²)	η (%)
Blank	-508	1.9	72	266	0.91		180.4	71	
0.5 mM	-490	1.7	250	156	0.89	69.6	103.5	208	65.7
1.0 mM	-485	1.5	282	151	0.89	75.9	102.7	278	74.3
5.0 mM	-484	1.9	308	150	0.90	76.8	106.2	294	75.7
10 mM	-475	1.7	494	136	0.91	85.4	102.9	500	85.7

C_{dl} values determined from CPE parameters, Y_o and n , as described in Ref. [43].

$$Z_{CPE} = [Y_o(jw)^n]^{-1} \quad (3)$$

Where j is the imaginary root, Y_o is the extent of the CPE, w is the angular frequency, and n ($-1 \leq n \leq 1$) is the diversion parameter with regard to the phase shift vanity the microscopic oscillation of the MS surface [44].

The efficiency of inhibition (η) % was determined using the following equation:

$$\eta\% = \left(\frac{R_p' - R_p}{R_p'} \right) \times 100 \quad (4)$$

Where R_p and R_p' are the polarization resistance with and without 2-HEI respectively. It was found that (η) improved with an increase in the 2-HEI concentration as seen Table 1 [45].

When we compared our study with the literature data, e.g. Wang et al. [46] studied the inhibition effect of aromatic imidazolidinone and its derivate. They found R_p and inhibition efficiency as 206.4 Ω cm² and 92.9%, at 25 mg L⁻¹ concentration of inhibitor in the 3.5 wt.% NaCl solutions. Yüce et al. [47] also investigated the inhibition performance of thiohydantoin derivate in 0.1 M HCl solution on MS. And they showed that the inhibition efficiency of this inhibitor was around 97% from the EIS results. In another study, Okafor et al. [48] measured the behaviors of inhibition of 2-undecyl-1-ethylamino imidazoline (2UEI) in 3% NaCl solutions. The inhibition efficiencies increased with the increasing of inhibitor concentration and reached 90.61% in

CO₂-saturated 3% NaCl solutions. Zhao and Chen [49] carried out the corrosion inhibition effects of oleic-based imidazoline (OIM) and sodium benzoate (SB) on MS in a CO₂-saturated solution. The results showed that, the compounds adsorbed in their protonated forms on the metal surface. Li and et al. [50] showed for a 3 g/L acetic acid (HAc), where 0.1 g/L imidazoline (IM) as a mixed-type inhibitor that R_p and inhibition efficiency is 99.4%, at N80 carbon steel in CO₂-saturated NaCl solution containing acetic acid. Moreover, Ikenna et al. [51] investigated the inhibition efficiencies of 5-(4-hydroxy3-methoxyphenyl)-2,7-dithio-2,3,5,6,7,8-hexahydro-pyrimido[4,5-d]pyrimidin-4(1H)-one (PP), in CO₂ corrosion was studied by means of electrochemical impedance spectroscopy (EIS) and potentiodynamic polarization (PDP) were complemented with scanning electron microscopy (SEM), techniques to assess the corrosion inhibition performance. They found the inhibition efficiency as 98%. Our impedance results will be improved and 2-HEI will support the literature studies by taking into account the physical and chemical meaning of the inhibition properties.

3.4. Adsorption isotherm

To utilize corrosion thermodynamic parameters and adsorption operations of MS in acidic environment, estimates were executed in the temperature range 20–50 °C in the presence and absence of inhibitor (in the case of 0.5 M HCl concentration of inhibitor is 10 mM), after 1 h of immersion.

Surface coverage degree (θ), for different concentrations of 2-HEI (C_{inh}) in 0.5 M HCl solution is obtained from EIS measurements and these data are applied to a suitable adsorption isotherm.

A straight line is yielded in the plot of C_{inh}/θ versus C_{inh} (Figure 6), thus calculated correlation coefficient is very close to unity. The slope is also very close to unity. Adsorption of 2-HEI from 0.5 HCl solution on the surface of MS corresponds to isotherm of Langmuir adsorption, which is presented by Eq. (5).

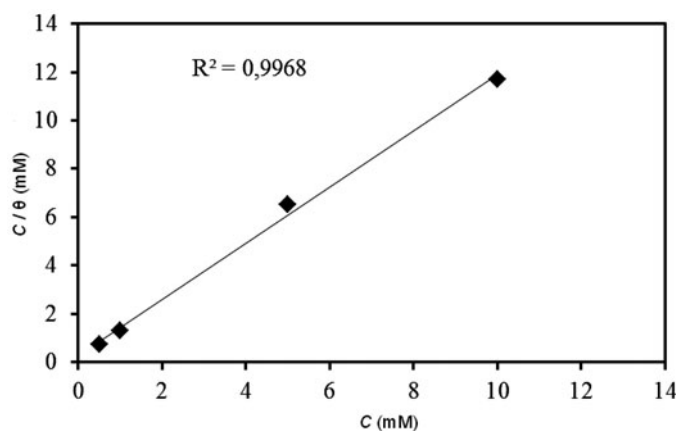


Figure 6. Langmuir adsorption plot of MS in 0.5 M HCl solution containing different concentrations of 2-HEI.

$$\frac{C_{\text{inh}}}{\theta} = \frac{1}{K_{\text{ads}}} + C_{\text{inh}} \quad (5)$$

The equilibrium constant value, K_{ads} of $38.12 \times 10^2 \text{ M}^{-1}$, demonstrates the high adsorption of 2-HEI on the surface of MS. The $\Delta G_{\text{ads}}^\circ$ on surface of MS can be determined with the following equation:

$$\Delta G_{\text{ads}}^\circ = -RT(\ln 55.5K_{\text{ads}}) \quad (6)$$

The calculated value of $\Delta G_{\text{ads}}^\circ$ is $-29.87 \text{ kJ mol}^{-1}$. The negative $\Delta G_{\text{ads}}^\circ$ value ensures strong and spontaneous adsorption of 2-HEI film on the MS surface. Generally, the magnitude of $\Delta G_{\text{ads}}^\circ$ up to -20 kJ mol^{-1} or less negative implies the electrostatic interactions exist between the charged molecules and the charged MS surface (physisorption). On the other hand, the magnitude around -40 kJ mol^{-1} or more negative indicates charge sharing or transfer from the inhibitor molecules to the MS surface (chemisorption) [45–56]. For this reason, the 2-HEI adsorption on the surface of MS includes both physisorption and chemisorption.

Figure 6 shows adsorption isotherm of Langmuir for 2-HEI on MS. A reasonable straight line is obtained ($r^2 = 0.99$) with a slope equal ≈ 1 2-HEI. The worth 55.5 in this situation is the concentration (M) of H_2O in solution [57]. This lean and negative values of $\Delta G_{\text{ads}}^\circ$ demonstrates spontaneous and presumably both physical and chemical inhibitor adsorption in 0.5 M HCl solution [58].

Electrostatic and/or donor acceptor interplay between vacant d-orbitals of Fe atoms at the surface and electron density of S and N atoms and aromatic ring molecules elucidates the adsorption of inhibitor structures on the MS surface [59,60].

3.5. Effect of temperature

In order to examine the temperature effect on inhibition performance of 2-HEI, EIS and PD measurements were fulfilled at various temperatures, ranging from 20 to 50 °C, in the absence and the presence of 10 mM 2-HEI after 1 h exposure. The obtained results are given in Table 2. As it is clear from Table 2, it is visible that the corrosion current densities increase in both without and with inhibitor and with the rising of temperature, and the inhibition efficiency decreases, showing that inhibition of 2-HEI is temperature-dependent [5]. The increasing E_a (%) with temperature suggests that the interactions of the inhibitor molecules with the surface of metal are more chemical than physical.

Table 2. Effect of temperature MS electrode obtained in 0.5 mol L⁻¹ HCl in the absence and presence of 10.0 mmol L⁻¹ 2-HEI solutions electrochemical parameters.

T(°C)	R_p ($\Omega \text{ cm}^2$)		CPE ($\times 10^6 \text{ s}^n \Omega^{-1} \text{ cm}^{-2}$)		η (%)
	Blank	2-HEI	Blank	2-HEI	
20	72	494	266	136	85.4
30	42	250	379	161	83.2
40	22	108	690	178	79.6
50	13	59	731	274	78.0

The value of E_a determined in the inhibited solution (56.8 kJ mol^{-1}) being higher than the value of E_a in the uninhibited solution (45.5 kJ mol^{-1}) shows that a physical (electrostatic) adsorption has occurred in the first stage [18,40].

Besides, the increase in E_a can be correlated with the increase in the thickness of the double layer [40]. But, the process of adsorption could not be graded as merely chemical or physical. Owing to competitive adsorption with H_2O structures, the adsorption criteria type acquired from the activation energy of change can not be taken as a stable. Hence, the adsorption of 2-HEI on the MS surface from HCl solution occurs by way of both chemical and physical transactions synchronically with largely first one [53].

In Figures 7 and 8, the EIS results in 0.5 M HCl solution with and without 10 mM 2-HEI were displayed, seriatim. The R_p , CPE acquired from fitted EIS datum and efficiencies of inhibition were epitomised in Table 2. The R_p values diminished slowly because of inhibitor release structures from the surface due to the temperature effect, which also proves adsorption of physical. The R_p values were estimated as $59 \Omega \text{ cm}^2$ and $13 \Omega \text{ cm}^2$ for inhibitor presence (in the case of 0.5 M HCl concentration of inhibitor is 10 mM) and uninhibitor conditions at 50°C , seriatim. As it is seemingly seen from Table 2, estimated efficiencies of inhibition remain considerably high (78%) even the highest temperature. Furthermore, many inhibitors replace with H_2O slowly with temperature in OHP, thus the CPE values tend to remain.

Figures 9 and 10 show the PD results in the uninhibitor and inhibitor at temperatures of 20°C , 30°C , 40°C and 50°C . As shown in Figure 9, the temperature has an important effect on both cathodic and anodic current values for the uninhibitor solution. In addition, the dissociation and hydrogen evolution reactions of MS dissociate faster with the current values. The anodic party as well exhibits change in the gradient with augmenting temperature. It is correlated to changed kinetics for passing between Fe^{3+} and Fe^{2+} ions [61]. As it is visible from Figure 10, the acquired valid values for either cathodic or anodic aspect are still lower than weighed in uninhibitor solution, beneath raised temperature conditions. The intimate cathodic and anodic reactions have exceedingly affected by the adsorbed inhibitor structures. Besides, the temperature in the inhibitors has a higher value with the cathodic. Increasing the temperature of the desorption process of inhibitory structures from the MS surface. This was previously explained by the interaction with the MS surface with strong adsorption. However, further enhance in the temperature decreases the affects of inhibitor in the interface, which indicate that inhibitor adsorption occurs fewer affirmative. In order to attain rate of corrosion from PD result sicorrand cathodic Tafel curves values were designated from Figures 9 and 10 which show cathodic reactions in the uninhibitor and inhibitor, including solutions at different temperatures. In addition, the i_{corr} values are indicated in the 2-HEI results at different temperatures. The estimated parameters of the corrosion approach each other with increasing temperature. The mechanism of inhibition was explicated from E_a values designated with assist of equation of Arrhenius, Eq. (7). However, the i_{corr} values gained from EIS results were salvaged to designate the E_a of corrosion. The acquired Arrhenius plot for MS in 0.5 M HCl in the presence and absence of inhibitor is expensed in Figure 11. The E_a value is based on the slope of these curves.

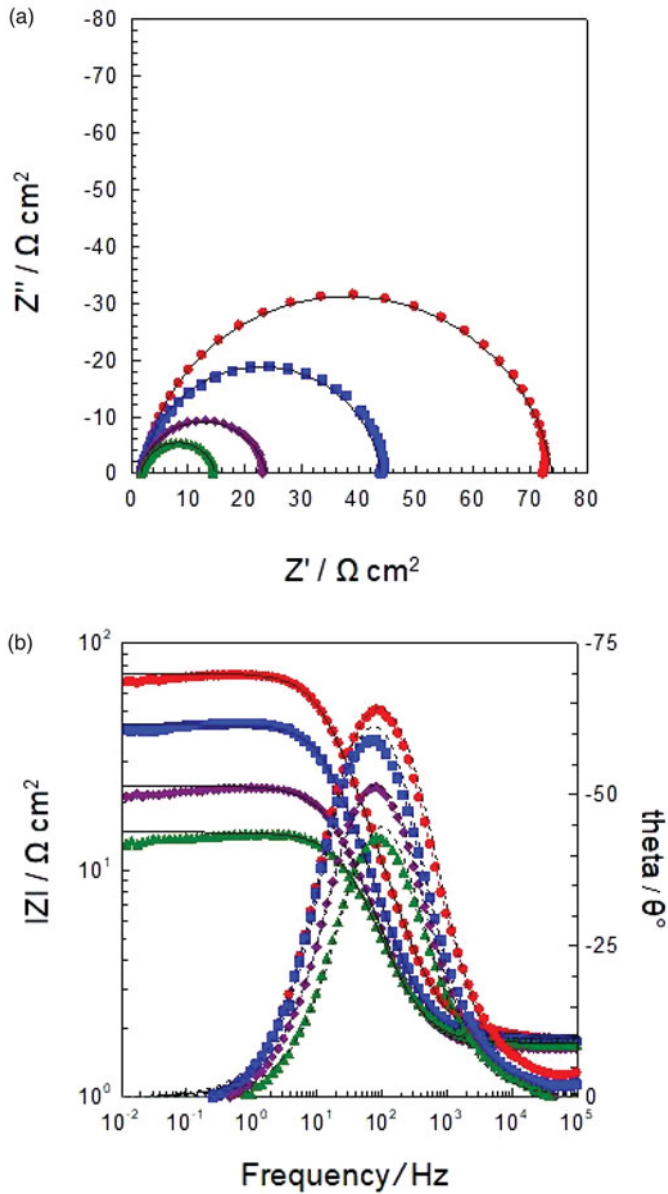


Figure 7. Nyquist plots of MS electrodes in 0.5 M HCl solution in the absence at different temperature (a) 20 °C (●), 30 °C (■), 40 °C (◆) and 50 °C (▲).

The E_a values were determined as 45.5 kJ mol^{-1} and 56.8 kJ mol^{-1} for uninhibitor and inhibitor conditions, respectively. When inhibitors are present, the decrease in E_a value is elucidated by the coordinated formation complexes of Fe^{2+} and inhibitor structures. 2-HEI structures are chemically adsorbed on the MS surface by complex formation with Fe^{2+} [62–64].

$$i_{\text{corr}} = A \exp(-E_a/RT) \quad (7)$$

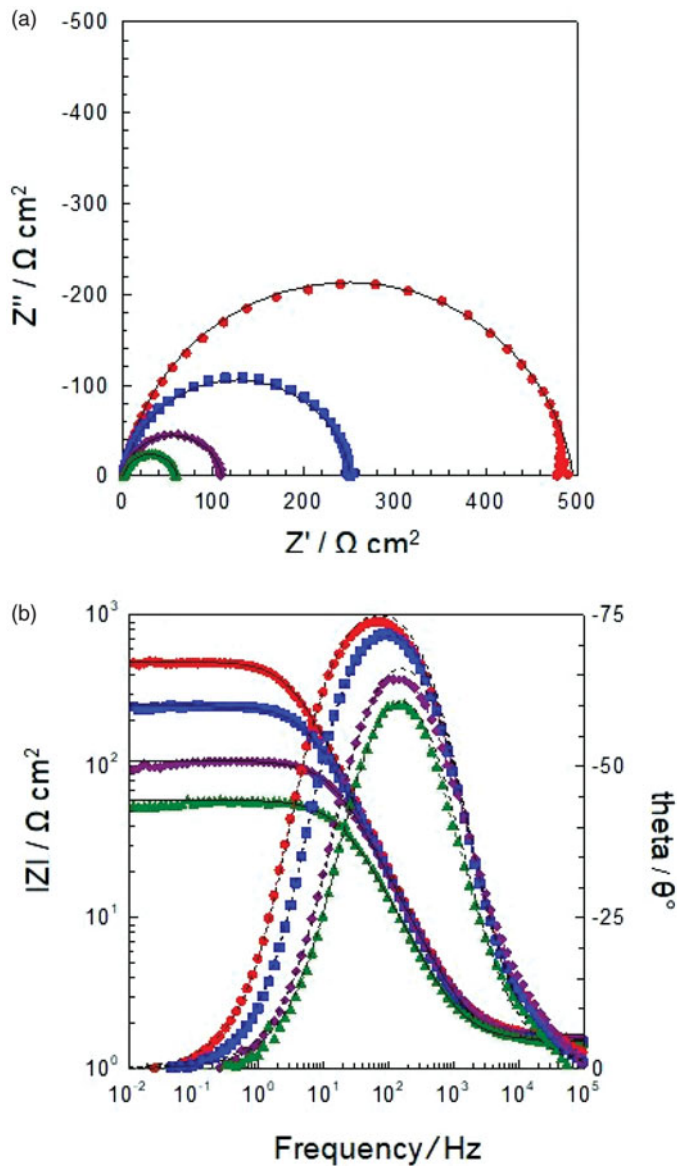


Figure 8. Nyquist plots of MS electrodes in 0.5 M HCl solution presence of 10.0 mM 2-HEI at different temperature 20 °C (●), 30 °C (■), 40 °C (◆) and 50 °C (▲) after fitted results.

3.7 SEM analysis

The surfaces of MS specimens in 0.5 M HCl solution without and with optimum concentration (10 mM) 2-HEI for 120 h exposure are given in Figure 12(a,b). As it is seen from Figure 12(a), the surface is highly damaged with lots of pits and cavities in the inhibitor absence, and this confirms MS dissolution in the aggressive medium. In Figure 12(b), the inhibited MS surface is smooth, no pits and cavities, and this confirms inhibition occurring on the MS surface. This improvement in surface protection

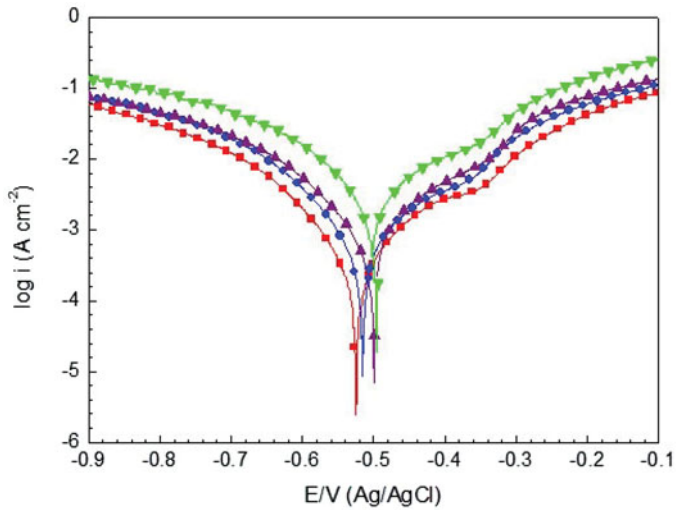


Figure 9. Potentiodynamic polarization curves of MS electrode obtained in 0.5 M HCl solution in the absence 20 °C (●), 30 °C (■), 40 °C (◆) and 50 °C (▲).

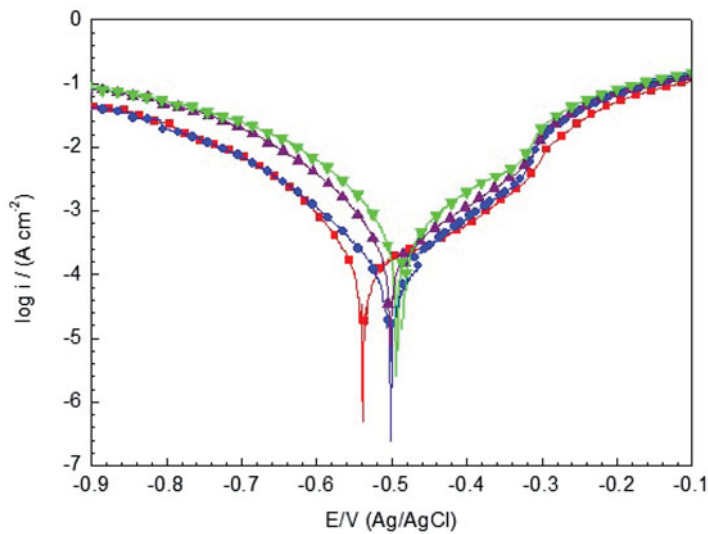


Figure 10. Potentiodynamic polarization curves of MS electrode obtained in 0.5 M HCl solution presence of 10.0 mmol L⁻¹ 2-HEI at different temperature 20 °C (●), 30 °C (■), 40 °C (◆) and 50 °C (▲).

is due to the formation of protective film or reduction of the rate of corrosion on the MS surface.

3.6. Theoretical calculations

Quantum chemical calculation of 1-(2-Hidroksietil)-2-İmidazolidion (2-HEI) was utilized to understand the relationship between the electronic properties of molecular structure and the corresponding inhibitive effect on the surface of metallic. **Figure 13**

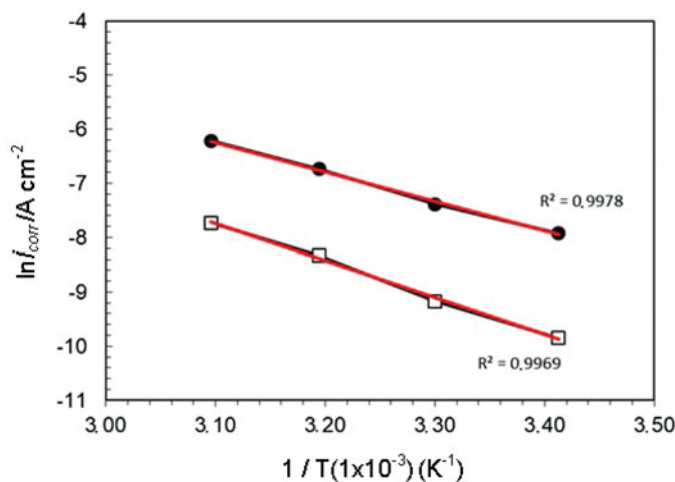


Figure 11. Arrhenius plots for the MS electrode in 0.5 M HCl (●) and containing 10.0 mmol L⁻¹ 2-HEI (□) solutions.

shows optimized geometry structures of HOMO and LUMO of the studied compound. According to Koopmans' theorem, the energy of E_{HOMO} is directly related to the ionization potential (I) while the energy of E_{LUMO} is directly related to the electron affinity (A) [65]. The geometrically optimized structure and electronic properties (E_{HOMO} , E_{LUMO} , Total energy, Dipole moment) were obtained by DFT/B3LYP/6-311G(++, d,p) method. Other quantum chemical parameters such as energy gap (ΔE), Total energy, Dipole moment (μ), global hardness (γ), softness (σ), and absolute electronegativity (χ) was calculated [66–70] and the results are presented in Table 3. The values determined in this study were 5.663 eV for band gap -0.645 eV for E_{LUMO} ; -6.308 for E_{HOMO} , respectively. These have demonstrated the high adsorption ability of 2-HEI. We have determined electronegativity, stiffness and softness to give more information about 2-HEI (Table 3). The values were 3.477 eV for electronegativity; 2.832 eV for hardness and 0.353 eV for softness respectively.

The Mulliken charge of atoms in inhibitor molecule is shown in Figure 13(a). The highest negative charge is located on oxygen, and this clearly indicates strong interaction occurring between ester oxygen and a metal ion. The HOMO value is higher in the zone to the oxygen and nitrogen (Figure 13(b)), which is attributed to the presence of a lone pair of electrons in the nitrogen and oxygen atoms of inhibitor. Therefore, the preferred active sites for donating electrons in the 2-HEI are mainly located in the regions around the oxygen and nitrogen atoms. The LUMO densities in the ring region were higher (Figure 13(c)), indicating the preferred active regions for accepting these electrons. Therefore, it is reasonable to assume that oxygen is donating electrons and forming a strong interaction with untreated d-orbitals of the metal, while the nitrogen in the protonated ring region accepts electrons from the metal surface containing the chloride ion.

Adsorption of an inhibitor on the MS surface may take place on the basis of donor-receptor interactions between the unshared-electrons of the heterocyclic compound

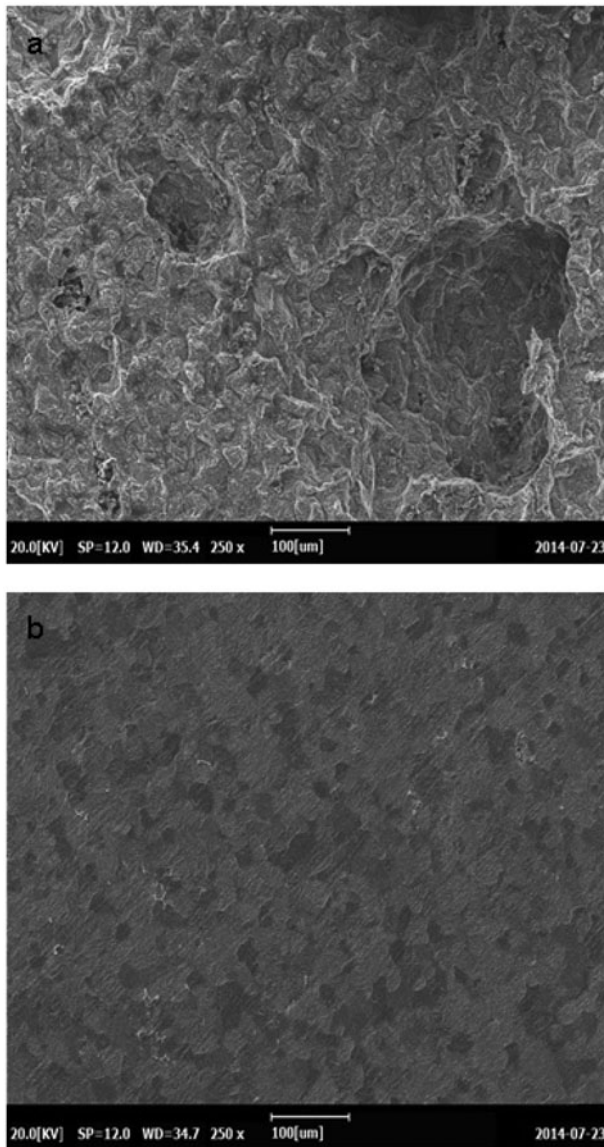


Figure 12. SEM images of MS samples: after immersion for 120 h (a) in 0.5 mM HCl solution without inhibitor and after immersion 120 h (b) in 0.5 M HCl solution in the presence of 10.0 mmol L⁻¹ 2-HEI.

and the empty d-orbitals of the MS surface atoms. Therefore, the energies of the boundary trajectories must be taken into account. The adsorption of 2-HEI on the surface of the MS as a neutral molecule can occur directly, including displacement of the water molecules from the MS surface and the sharing of electrons between the nitrogen atoms and the surface of the MS. Also we may emphasize that N containing heterocyclic inhibitor compounds most probably adsorb on MS surface (physisorption) in horizontal position, in 2HEI two N atoms may direct molecule such as a blanket on MS surface and cover surface like an inhibitor film. Most probably these events are

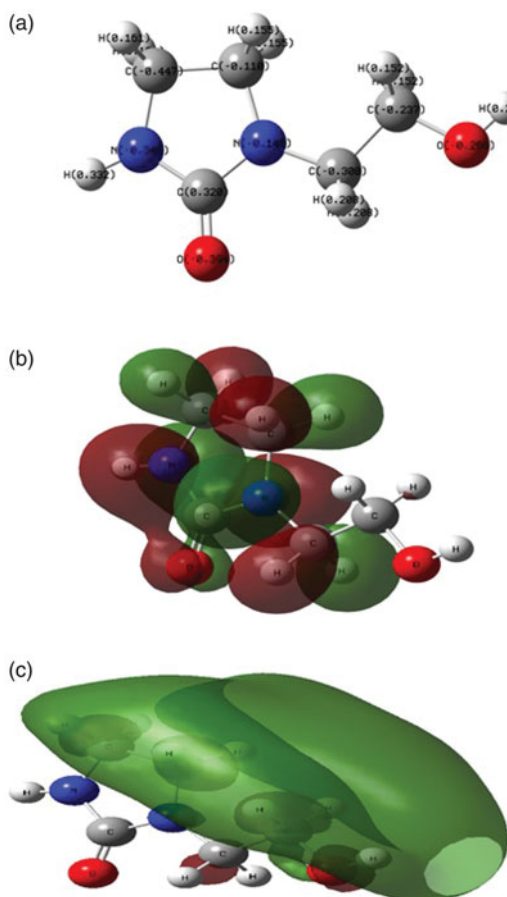


Figure 13. Optimized molecular structures of 2-HEI. with Mulliken charge (a), HOMO (b) and LUMO (c) orbitals.

Table 3. The calculated quantum parameters for 2-HEI by DFT/B3LYP/6-311G (++, d,p) method in water phase.

Inhibitor	E_{HOMO} (eV)	E_{LUMO} (eV)	ΔE (eV)	β (eV)	γ (eV)	s (eV ⁻¹)
2-HEI	-6.308	-0.645	5.663	3.477	2.832	0.353

E_{HOMO} : Energy of the highest occupied molecular orbital.

E_{LUMO} : Energy of the lowest unoccupied molecular orbital.

ΔE : Energy gap between LUMO and HOMO.

β : electronegativity.

γ : global hardness.

s : global softness.

done physical interaction which is evident in from the value of $\Delta G^{\circ}_{\text{ads}}$ obtained. So we may say that comparison of theoretical HOMO and LUMO energy band gap and experimental adsorption data correlate each other. Furthermore it proves literature findings which offer physical adsorption of 2-HEI derivatives. Not only physical but also some chemical interactions may occur on metal surface in outer Helmholtz layer. The main idea in inhibitor applications is development of inhibitor barrier layer/film/accumulation between metal and corrosive medium. And the protection of the

inhibitor molecule increases with increasing adsorption energy and adsorption layer. Some times first layer of adsorption may occur with dominant effect of chemical interactions but other layer may interact as physical and accumulation on the surface may protect surface and push the corrosive specimens out from the metal surface. In this study we proved that experimental data were correlated via quantum chemical calculations.

4. Conclusions

From the current work, the following points can be concluded:

1. The EIS results indicated that MS was prevented from dissolving of MS surface by adsorption of 2-HEI. EIS results displayed that the corrosion rate diminished since strong adsorption features of 2-HEI molecules on the MS surface by way of electronegative nitrogen, oxygen atoms and electron rich rings. The 2-HEI compound studied are good inhibitors for MS in 0.5 M HCl. The efficiency of inhibition increases with the inhibitor concentration.
2. The addition of 2-HEI causes a decrease in both cathodic and anodic currents. The corrosion potential (E_{corr}) of 2-HEI was observed to shift towards more noble potentials with increasing additive concentration, indicating the inhibitors to be of anodic character and formation of a surface film.
3. The adsorption behaviour of 2-HEI confirmed to the isotherm of Langmuir adsorption and included adsorption, both physical adsorption and chemical adsorption.
4. The negative value of $\Delta G^{\circ}_{\text{ads}}$ showed that the adsorption of inhibitor molecules on the surface of MS is spontaneous. The $\Delta G^{\circ}_{\text{ads}}$ value, $-29.87 \text{ kJ mol}^{-1}$, displayed that 2-HEI interacted with the MS surface by way of chemical type adsorption behavior, regulation with vacant d-orbitals of Fe atoms. Moreover, temperature works showed that efficiencies of inhibition were high (78%) even at the highest temperatures.
5. SEM exhibited a uniform smooth surface formation on the MS with inhibitor, indicating the formation of a good protective layer on the MS surface. The powerful interaction between 2-HEI and MS surface was also sighted from SEM pictures even after 120 h early fallout.
6. This study shows that theoretical calculations are suitable for experimental electrochemical observations.

Disclosure statement

No potential conflict of interest was reported by the authors.

Funding

This study is supported by a grant from Scientific Research Projects Committee of Çukurova University and Mardin Artuklu University (MAÜ-BAP-16-SYO-06).

References

- [1] Abd El Rehim SS, Ibrahim MAM, Khalid KF. The inhibition of 4-(2'-amino-5'-methylphenylazo) antipyrine on corrosion of mild steel in HCl solution. *Mater Chem Phys.* 2001;70:268–273.
- [2] Oguzie EE, Unaegbu C, Ogukwe CN, et al. Inhibition of mild steel corrosion in sulphuric acid using indigo dye and synergistic halide additives. *Mater Chem Phys.* 2004; 84:363–368.
- [3] Patel N, Beranek P, Nebyla M, et al. Inhibitive effects by some benzothiazole derivatives on mild steel corrosion in 1 N HCl. *Int J Electrochem Sci.* 2014;9:3951–3960.
- [4] Bentiss F, Lebrini M, Lagrene M. Thermodynamic characterization of metal dissolution and inhibitor adsorption processes in mild steel/2,5-bis(n-thienyl)-1, 3,4-thiadiazoles/hydrochloric acid system. *Corros Sci.* 2005;47:2915–2931.
- [5] Tang YM, Zhang F, Hu SX, et al. Novel benzimidazole derivatives as corrosion inhibitors of mild steel in the acidic media. Part I: gravimetric, electrochemical, SEM and XPS studies. *Corros Sci.* 2013;74:271–282.
- [6] Aljourani J, Raeissi K, Golozar MA. Benzimidazole and its derivatives as corrosion inhibitors for mild steel in 1M HCl solution. *Corros Sci.* 2009;51:1836–1843.
- [7] F Bentiss, Ch. Jama, B Mernari, H El Attari, et al. Corrosion control of mild steel using 3,5-bis(4-methoxyphenyl)-4-amino-1,2,4-triazole in normal hydrochloric acid medium. *Corros Sci.* 2009;51:1628–1635.
- [8] Hassan HH, Abdelghani E, Amin MA. Inhibition of mild steel corrosion in hydrochloric acid solution by triazole derivatives Part I. Polarization and EIS studies. *Electrochim Acta.* 2007;52:6359–6366.
- [9] Abboud Y, Abourriche A, Saffaj T, et al. The inhibition of mild steel corrosion in acidic medium by 2,20-bis(benzimidazole). *Appl Surf Sci.* 2006;252:8178–8184.
- [10] Singh AK, Quraishi MA. The effect of some bis-thiadiazole derivatives on the corrosion of mild steel in hydrochloric acid. *Corros Sci.* 2010;52:1373–1385.
- [11] Ju H, Kai Z, Li Y. Aminic nitrogen-bearing polydentate Schiff base compounds as corrosion inhibitors for iron in acidic media: a quantum chemical calculation. *Corros Sci.* 2008;50:865–871.
- [12] Li XH, Deng SD, Fu H, et al. Corrosion inhibition of Cresol red for cold rolled steel in phosphoric acid solution. *Corros. Sci Prot Technol.* 2009;21:354–357.
- [13] Sathiyabama J, Rajendran S, Solvi JA, et al. Methyl orange as corrosion inhibitor for carbon steel in well water. *Indian J Chem Technol.* 2008;15:462–466.
- [14] Ebsenso EE, Alemu H, Umoren SA, et al. Inhibition of mild steel corrosion in sulphuric acid using alizarin yellow GG dye and synergistic iodide additive. *Int J Electrochem Sci.* 2008;3:1325–1339.
- [15] Prabhu RA, Venkatesha TV, Shanbhag AV. Carmine and fast green as corrosion inhibitors for mild steel in hydrochloric acid solution. *JICS.* 2009;6:353–363.
- [16] Ashassi-Sorkhabi H, Seifzadeh D, Hosseini MG. EN, EIS and polarization studies to evaluate the inhibition effect of 3H-phenothiazin-3-one, 7-dimethylamin on mild steel corrosion in 1 M HCl solution. *Corros Sci.* 2008;50:3363–3370.
- [17] Li XH, Deng SD, Fu H. Inhibition effect of methyl violet on the corrosion of cold rolled steel in 1.0 M HCl solution. *Corros Sci.* 2010;52:3413–3420.
- [18] Xu B, Liu Y, Yin XS, et al. Experimental and theoretical study of corrosion inhibition of 3-pyridincarbozalde thiosemicarbazone for mild steel in hydrochloric acid. *Corros Sci.* 2013;74:206–213.
- [19] Wang L. Inhibiting effect of 2-mercaptopyrimidine on the corrosion of a low carbon steel in phosphoric acid. *Corros Sci.* 2001;43:1637–1644.
- [20] Abdallah M, Helal EA, Fouda AS. Aminopyrimidine derivatives as inhibitors for corrosion of 1018 carbon steel in nitric acid solution. *Corros Sci.* 2006;48:1639–1654.
- [21] Çalışkan N, Akbaş E. The inhibition effect of some pyrimidine derivatives on austenitic stainless steel in acidic media. *Mater Chem Phys.* 2011;16:983–988.

- [22] Khaled KF. Studies of the corrosion inhibition of copper in sodium chloride solutions using chemical and electrochemical measurements. *Mater Chem Phys.* 2011;125:427–433.
- [23] Mert BD, Yüce AO, Kardaş G, et al. Inhibition effect of 2-amino-4-methylpyridine on mild steel corrosion: experimental and theoretical investigation. *Corros Sci.* 2014;85:287–295.
- [24] Masoud MS, Awad MK, Shaker MA, et al. The role of structural chemistry in the inhibitive performance of some aminopyrimidines on the corrosion of steel. *Corros Sci.* 2010;52:2387–2396.
- [25] Patru Samide A, Bibicu I. Kinetics corrosion process of carbon steel in hydrochloric acid in absence and presence of 2-(cyclohexylaminomercapto)benzothiazole. *Surf Interface Anal.* 2008;40:944–952.
- [26] Popova A, Christov M, Vasilev A. Mono- and dicationic benzothiazolic quaternary ammonium bromides as mild steel corrosion inhibitors. Part II: electrochemical impedance and polarisation resistance results. *Corros Sci.* 2011;53:1770–1777.
- [27] Moretti G, Quartarone G, Tassan A, et al. 5-Amino- and 5-chloro-indole as mild steel corrosion inhibitors in 1 N sulphuric acid. *Electrochim Acta.* 1996;41:1971.
- [28] Soltani N, Tavakkoli N, Khayatkashani M, et al. Green approach to corrosion inhibition of 304 stainless steel in hydrochloric acid solution by the extract of *Salvia officinalis* leaves. *Corros Sci.* 2012;62:122–135.
- [29] Kelly RG, Scully JR, Shoesmith DW, et al. *Electrochemical techniques in corrosion science and engineering (127290–127302)*. New York (NY): Marcel Dekker Inc.; 2003.
- [30] Hosseini M, Fotouhi L, Ehsani A, et al. Enhancement of corrosion resistance of polypyrrole using metal oxide nanoparticles: potentiodynamic and electrochemical impedance spectroscopy study. *J Col Inter Sci.* 2017;505:213–219.
- [31] Ehsania A, Ghasem Mahjani M, Moshrefi R, et al. Electrochemical and DFT study on the inhibition of 316L stainless steel corrosion in acidic medium by 1-(4-nitrophenyl)-5-amino-1H-tetrazole. *RSC Adv.* 2014;38:20031–20037.
- [32] Martinez S, Metikos-Hukovic M. A nonlinear kinetic model introduced for the corrosion inhibitive properties of some organic inhibitors. *J Appl Electrochem.* 2003;33:1137–1142.
- [33] Bentiss F, Traisnel M, Gengembre L, et al. A new triazole derivative as inhibitor of the acid corrosion of mild steel. *Appl Surf Sci.* 1999;152:237–249.
- [34] Gholizadeh-Gheshlaghi M, Seifzadeh D, Shoghi P, et al. Electroless Ni-P/nano-WO₃ coating and its mechanical and corrosion protection properties. *J Alloys Comp.* 2018;769:149–160.
- [35] Lece HD, Emregul KC, Atakol O. Difference in the inhibitive effect of some Schiff base compounds containing oxygen, nitrogen and sulfur donors. *Corros Sci.* 2008;50:1460–1468.
- [36] Quraishi MA, Rawat J. Influence of iodide ions on inhibitive performance of tetraphenyl-dithia-octaaza-cyclotetradeca-hexaene (PTAT) during pickling of mild steel in hot sulfuric acid. *Mater Chem Phys.* 2001;70:95–99.
- [37] Yıldız R, Doğan T, Dehri İ. Evaluation of Corrosion Inhibition of Mild Steel in 0.1 M HCl by 4-Amino-3-Hydroxynaphthalene-1-Sulphonic Acid. *Corros Sci.* 2014;85:215–221.
- [38] Erbil M. Determination of corrosion rates by analysis of AC impedance diagrams. *Chim Acta Turc.* 1988;1:59–70.
- [39] Ongun Yuce A, Kardaş G. Adsorption and inhibition effect of 2-thiohydantoin on mild steel corrosion in 0.1 M HCl. *Corros Sci.* 2012;58:86–94.
- [40] Solmaz R, Kardaş G, Çulha M, et al. Investigation of adsorption and inhibitive effect of 2-mercapto thiazoline on corrosion of mild steel in hydrochloric acid media. *Electrochim Acta.* 2008;53:5941–5952.

- [41] Kowsari E, Arman SY, Shahini MH, et al. In situ synthesis, electrochemical and quantum chemical analysis of an amino acid-derived ionic liquid inhibitor for corrosion protection of mild steel in 1M HCl solution. *Corros Sci.* 2016;112:73–85.
- [42] Raistrick ID, Franceschetti DR, Macdonald JR. Impedance spectroscopy theory, experiment, and application. 2nd ed. Hoboken (NJ): John Wiley & Sons Inc.; 2005.
- [43] Hsu CH, Mansfeld F. Technical note: concerning the conversion of the constant phase element parameter Y_0 into a capacitance. *Corros Sci.* 2001;57:747–748.
- [44] Qiang Y, Zhang S, Tan B, et al. Evaluation of Ginkgo leaf extract as an eco-friendly corrosion inhibitor of X70 steel in HCl solution. *Corros Sci.* 2018;133:6–16.
- [45] Yıldız R. An electrochemical and theoretical evaluation of 4,6-diamino-2-pyrimidine-thiol as a corrosion inhibitor for mild steel in HCl solutions. *Corros Sci.* 2015;9: 544–553.
- [46] Wang D, Xiang Liang BY, Song S, et al. Corrosion control of copper in 3.5 wt.% NaCl Solution by Domperidone: experimental and Theoretical Study. *Corros Sci.* 2014;85: 77–86.
- [47] Yüce AO, Telli E, Mert BD, et al. Experimental and quantum chemical studies on corrosion inhibition effect of 5,5 diphenyl 2-thiohydantoin on mild steel in HCl solution. *Corros Sci.* 2016;218:384–392.
- [48] Okafor PC, Liu X, Zheng YG. Corrosion inhibition of mild steel by ethylamino imidazoline derivative in CO₂-saturated solution. *Corros Sci.* 2009;51:761–768.
- [49] Zhao J, Chen G. The synergistic inhibition effect of oleic-based imidazoline and sodium benzoate on mild steel corrosion in a CO₂-saturated brine solution. *Electrochim Acta.* 2012;69:24–255.
- [50] Li YZ, Xu N, Guo XP, Zhang GA. Inhibition effect of imidazoline inhibitor on the crevice corrosion of N80 carbon steel in the CO₂-saturated NaCl solution containing acetic acid. *Corros Sci.* 2017;126:127–141.
- [51] Onyeachu IB, Quraishi MA, Obot IB, et al. Newly synthesized pyrimidine compound as CO₂ corrosion inhibitor for steel in highly aggressive simulated oilfield brine. *J Adhe Sci Techno.* 2019;33:1226–1247.
- [52] Yıldız R, Döner A, Doğan T, et al. Experimental studies of 2-pyridinecarbonitrile as corrosion inhibitor for mild steel in hydrochloric acid solution. *Corros Sci.* 2014;82: 125–132.
- [53] Seifzadeh D, Basharnavaz H, Bezaatpour A. A Schiff base compound as effective corrosion inhibitor for magnesium in acidic media. *Mater Chem Phys.* 2013;138:794–802.
- [54] Seifzadeh D, Valizadeh-Pashabeigh V, Bezaatpour A. 5-CM-Salophen Schiff Base as an Effective Inhibitor for Corrosion of Mild Steel in 0.5 M HCl. *Chem Eng Com.* 2016; 203:1279–1287.
- [55] Seifzadeh D, Bezaatpour A, Joghani RA. Asadpour Joghani, Corrosion inhibition effect of N, N'-bis (2-pyridylmethylidene)-1,2-diiminoethane on AZ91D magnesium alloy in acidic media. *Trans Nonferrous Met Soc China.* 2014;24:3441–3451.
- [56] Seifzadeh D, Hamzedoust-Hasankiadeh S, Shamkhali AN. Electrochemical and Dft Studies of 8-hydroxyquinoline as Corrosion Inhibitor For AZ61 Magnesium Alloy In Acidic Media. *Prot Met Phys Chem Surf.* 2013;49:229–239.
- [57] Flis J, Zarkoczymski T. Impedance Study of Reinforcing Steel in Simulated Pore Solution with Tannin. *J Electrochem Soc.* 1996;143:2458–2464.
- [58] TrabANELLI G. In: Mansfield F, editor. Corrosion mechanism. New York (NY): Marcel Dekker; 1987, p. 18.
- [59] Murakawa T, Nagaura S, Hackermann N. A transition state of corrosion inhibition mechanism from adsorption to film forming. *Corros Sci.* 1968;7:433–435.
- [60] Bentiss F, Traisnel M, Lagrenee M. Inhibition of acidic corrosion of mild steel by 3,5-diphenyl-4H-1,2,4-triazole. *Appl Surf Sci.* 2000;161:194.
- [61] O'M. Bockris J, Reddy AKN, Gamboa-Aldeco M. Modern electrochemistry. 2nd ed. New York (NY): Kluwer Academic/Plenum Publishers; 2000.

- [62] Tang Y, Yang X, Yang W, et al. Experimental and molecular dynamics studies on corrosion inhibition of mild steel by 2-amino-5-phenyl-1,3,4-thiadiazole. *Corros Sci.* 2010;52:242–249.
- [63] Tansuğ G, Kicir N, Demirkol O, et al. Synthesis and application of phenylcarbamo-dithioate compound for steel protection. *J Adhes Sci Technol.* 2016;30:1984–2000.
- [64] Shaban SM, Aiad I, El-Sukkary MM, et al. Evaluation of some cationic surfactants based on dimethylaminopropylamine as corrosion inhibitors. *J Ind Eng Chem.* 2015;21:1029–1038.
- [65] John S, Joseph A. Electro analytical, surface morphological and theoretical studies on the corrosion inhibition behavior of different 1,2,4-triazole precursors on mild steel in 1 M hydrochloric acid. *Mater Chem Phys.* 2012;133:1083–1091.
- [66] Radilla J, Negrón-Silva GE, Palomar-Pardavé M, et al. DFT study of the adsorption of the corrosion inhibitor 2-mercaptoimidazole onto Fe(1 0 0) surface. *Electrochim Acta.* 2013;112:577–586.
- [67] Xavier RJ, Dinesh P. Spectroscopic (FTIR, FT-Raman, ^{13}C and ^1H NMR) investigation, molecular electrostatic potential, polarizability and first-order hyperpolarizability, FMO and NBO analysis of 1-methyl-2-imidazoethiol. *Spectrochim Acta A Mol Biomol Spectrosc.* 2014;118:999–1011.
- [68] Morsi RE, Khamis EA, Al-Sabagh AM. Polyaniline nanotubes: facile synthesis, electrochemical, quantum chemical characteristics and corrosion inhibition efficiency. *J Taiwan Inst Chem E.* 2016;60:573–581.
- [69] Yıldız R. Adsorption and inhibition effect of 2,4-diamino-6-hydroxypyrimidine for mild steel corrosion in HCl medium: experimental and theoretical investigation. *Ionics.* 2019;25:859–870.
- [70] Yıldız R, Doğru Mert B. Theoretical and Experimental Investigations on Corrosion Control of Mild Steel in Hydrochloric Acid Solution by 4-aminothiophenol. *Anti-Corros Meth Mater.* 2019;66:127–137.